Solid-State ^{13}C Chemical Shift Tensors in Terpenes. 2. NMR Characterization of Distinct Molecules in the Asymmetric Unit and Steric Influences on Shift in Parthenolide

James K. Harper, Gary McGeorge, and David M. Grant*

Contribution from the Department of Chemistry, University of Utah, Salt Lake City, Utah 84112

Received January 25, 1999. Revised Manuscript Received May 25, 1999

Abstract: PHORMAT and FIREMAT solid-state NMR analyses provide all of the ^{13}C tensor principal values for the carbons in solid parthenolide which contains two molecules per asymmetric crystallographic unit and 15 carbons per molecule. Only one pair of the isotropic lines is degenerate, thus 29 different sets of principal values have been measured along with the 29 isotropic resonances. The FIREMAT signal-to-noise per unit time is significantly higher than PHORMAT thereby allowing a more accurate ^{13}C tensor analysis in an experiment taking much less time. This FIREMAT feature is especially beneficial for the inherently broader sp^2 carbon spectral bands. Comparison of experimental tensor principal values with those computed from X-ray coordinates provides shift assignments for all carbon pairs. This comparison also clearly differentiates between shifts arising from the two specific molecules in the asymmetric unit for 7 of the 15 pairs of carbons. Two additional pairs of carbons may be assigned to specific molecules in the asymmetric unit at lower confidence levels while the six remaining carbon pairs (1 sp^2 and 5 sp^3) are unassignable in the asymmetric unit with the present level of theoretical computations. Experimental sp^2 and sp^3 principal values are used to evaluate five different tensor computational methods. The B3PW91 method with the 6-31+G (2d, p) basis provides the most accurate tensors with a root-mean-square error of 2.3 and 3.2 ppm for sp^3 and sp^2 carbons, respectively. Repulsive steric interactions between methyl protons and proximate neighboring protons correlate with large upfield shifts in two of the three methyl carbon tensor principal components. These changes appear to correlate with variations in the electronic charge in the $C-CH_3$ bond resulting from steric interactions.

Introduction

The NMR chemical shift has proven to be an unusually powerful tool in establishing details of molecular structure. While the preponderance of effort has been focused on experiments providing isotropic chemical shifts, the mathematical formulation that most accurately describes the chemical shift is a symmetrical second rank tensor with six potentially observable values.[1] Thus, focus only on isotropic shifts neglects structurally sensitive information contained in shift tensors.

Individual tensor components are unmeasurable in liquids as rapid molecular tumbling averages these components to a single isotropic shift. In solids, however, several methods have been developed for obtaining tensor components.[2] For powder samples, only the three principal values or components of the diagonalized tensor may be observed. These values are provided by the magic angle slow turning 2D PHORMAT experiment,[3] but unfortunately, PHORMAT analysis of relatively wide powder patterns (e.g., sp^2 hybridized carbons with widths of over 200 ppm) suffers from low signal to noise (S/N). To overcome some of these limitations the 2D FIREMAT experiment, also a magic angle slow turning experiment, has recently been developed.[4]

As with PHORMAT, the FIREMAT experiment provides anisotropic chemical shift powder patterns for individual carbons that have been separated in the second dimension by their isotropic shifts. In contrast to the near static patterns provided by PHORMAT, however, the increased spinning speed used in the FIREMAT analysis results in spinning sideband manifolds for each carbon. Concentrating the powder pattern intensities into sets of spinning sidebands provides greater S/N than can be obtained from comparable PHORMAT analysis. Increased FIREMAT S/N also is a consequence of the 5-π type of magic angle turning (MAT) experiment used and the inclusion of a novel data-replication technique.[4] As the near static patterns of PHORMAT are preferable in obtaining all *three* principal values when S/N is not an issue, the two methods may be used in a complementary manner.

The FIREMAT and PHORMAT experiments also include two additional improvements. First, the processing of evolution data uses the recently introduced TIGER technique.[5] TIGER processing collapses 2D experimental MAT data into a collection of 1D acquisition slices at selected isotropic frequencies by using a least-squares analysis. This isotropic information is obtained independently from separate 1D evolution spectra which are obtained either from a CP/MAS spectrum[6] or from Gan's pseudo 2D spinning sideband (P2DSS) replicated FIREMAT data.[7] The TIGER derived FID's may be directly Fourier transformed into

(1) Grant, D. M. In *Encyclopedia of NMR*; Grant, D. M., Harris, R. K., Eds.; Wiley: Chichester, 1996; Vol. 2, pp 1298−1321.
(2) Orendt, A. M. In *Encyclopedia of NMR*; Grant, D. M., Harris, R. K., Eds.; Wiley: Chichester, 1996; Vol. 2, pp 1282−1297.
(3) Hu, J. Z.; Wang, W.; Liu, F.; Solum, M. S.; Alderman, D. W.; Pugmire, R. J.; Grant, D. M. *J. Magn. Reson.* **1995**, *113*, 210.
(4) Alderman, D. W.; McGeorge, G.; Hu, J. Z.; Pugmire, R. J.; Grant, D. M. *Mol. Phys.* **1998**, *95*, 1113.
(5) McGeorge, G.; Hu, J. Z.; Mayne, C. L.; Alderman, D. W.; Pugmire, R. J.; Grant, D. M. *J. Magn. Reson.* **1997**, *129*, 134.
(6) Harper, J. K.; McGeorge, G.; Grant, D. M. *Magn. Reson. Chem.* **1998**, *36*, S135.
(7) Gan, Z. J. *Magn. Reson.* **1994**, *109*, 253.

10.1021/ja990251b CCC: $18.00
Published on Web 06/25/1999

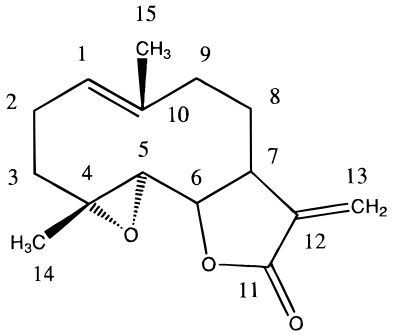

Figure 1. Structure of parthenolide.

1D tensor powder patterns. Hence, TIGER analysis greatly reduces the number of evolution increments required to achieve a given resolution and provides a significant improvement in total analysis time for all MAT spectra. Further, TIGER accommodates the unique phase and replication characteristics of the FIREMAT data.[4,5] The second improvement in both the PHORMAT and FIREMAT analyses was the inclusion of TPPM $^{13}C-\{^1H\}$ decoupling.[8] This modification yields significantly narrower lines thereby further improving the S/N.[6]

In this paper we describe application of both PHORMAT and FIREMAT analyses to the terpene parthenolide (structure shown in Figure 1) to obtain all shift tensors. Having determined tensors from both methods, the two sets of principal values may be compared statistically to estimate the precision in our tensor measurements. Chemical shift assignments are made by comparing experimental principal values with ab initio calculated tensors. Not only are these assignments given for all carbons, but it is shown for the first time that the majority of carbons may be assigned to one or the other of the two distinct molecules in the crystallographic asymmetric unit. Finally, a characterization of steric effects on methyl principal values, arising from perturbed methyl protons, is given.

Experimental Section

The liquid 2D INADEQUATE spectrum of parthenolide was acquired on a 500 MHz Varian Unity Plus spectrometer at 26 °C. The sample consisted of 97 mg in 0.7 mL of $CDCl_3$. The spectrum was referenced to the central line of $CDCl_3$ at 77.23 ppm. The INADEQUATE analysis used a 15 μs 90° ^{13}C pulse, a 7 s recycle time, and spectral widths of 23.9 kHz in both dimensions; the pulse sequence delay was optimized for detecting 55 Hz carbon−carbon scalar coupling constants. A total of 64 evolution increments of 64 transients each were collected for an analysis time of 7.9 h. Digital resolution for the F1 and F2 dimensions was 372.9 and 0.7 Hz per point, respectively. Spectral processing and chemical shift assignment were performed in a semiautomated fashion with use of previously described software.[9]

The ^{13}C PHORMAT spectrum[3] was acquired on a Chemagnetics CMX400 NMR spectrometer using a 7.5 mm PENCIL probe with a sample spinning speed of 30 Hz. The carbon frequency was 100.6202 MHz. Additional spectrometer parameters included a recycle time of 10 s, a 3.75 μs ^1H 90° pulse, a 3.8 μs ^{13}C 90° pulse, a contact time of 3 ms, a ^1H decoupling frequency of 400.1237 MHz, and spectral widths of 17.5 and 59.9 kHz in the evolution and acquisition dimensions, respectively. A total of 167 evolution increments of 256 transients each required an acquisition time of 228 h. TPPM proton decoupling[8] was used with a total phase-modulation angle of 16° together with a modulation frequency corresponding to a 180° tip angle. The acquisition dimension digital resolution was 116.9 Hz per point. TIGER processing eliminates the requirement of a Fourier transformation of the evolution dimension and achieves high resolution with shorter evolution times. Hence, the digital resolution of the PHORMAT evolution dimension reflects that of the 1D guide spectrum (described below) used to create the least-squares models for TIGER analysis.[5]

A high-resolution TPPM decoupled, CP/MAS isotropic 1D ^{13}C spectrum of parthenolide provided the guide for TIGER analysis of the PHORMAT data. The TOSS pulse sequence[10] employed a sample spinning speed of 4 kHz and the acquired digital resolution was 9.8 Hz per point. Other parameters are summarized in the description of the PHORMAT experiment.

The ^{13}C FIREMAT data were collected on the same 7.5 mm PENCIL probe and Chemagnetics CMX400 NMR spectrometer. A sample spinning speed of 1000 ± 0.5 Hz was used together with the pulse sequence recently described.[4] The TPPM proton decoupling worked best with a total phase-modulation angle of 20° and a modulation frequency corresponding to a 180° tip angle. Other parameters include a recycle time of 10 s, a 3.9 μs ^1H 90° pulse, a 8.0 μs 180° ^{13}C pulse, a contact time of 3 ms, a ^1H decoupling frequency of 400.1237 MHz, and spectral widths of 16.0 and 96.0 kHz in the evolution and acquisition dimensions, respectively. The analysis required 34 h and consisted of 16 evolution increments of 768 transients each. An extended evolution dimension with a digital resolution of 11.8 Hz per point was created by replicating and rearranging blocks of acquisition data as previously described.[4,7] The digital resolution of the acquisition dimension was 11.7 Hz per point. The high-frequency peak of adamantane at 38.4 ppm was used for referencing and setting the Hartman−Hahn match.

The 1D ^{13}C isotropic guide spectrum required for TIGER analysis was derived directly from the FIREMAT data by Fourier transforming the evolution points corresponding to the first acquisition point according to Gan's P2DSS suppression method.[4,7] The isotropic spectrum had a digital resolution of 11.8 Hz per point.

Parthenolide was obtained from Aldrich and used as received.

Results and Discussion

FIREMAT and PHORMAT Principal Shift Values. As this is the first use of the FIREMAT technique to solve a chemical problem, it is important that differences relative to previous methodologies (e.g., PHORMAT) be evaluated to verify the accuracy and usefulness of this new method. Here FIREMAT is shown to improve upon earlier MAT methods in terms of S/N and time savings and to give comparable accuracy for derived tensor values.

The isotropic spectrum of parthenolide contains 29 lines for the 15 carbons present. This doubling of all but one line, which was accidentally degenerate, is consistent with the presence of 2 molecules per asymmetric unit as found by X-ray analysis.[11] Minor structural and environmental differences between the two molecules give rise to the observed spectral doubling. The FIREMAT and PHORMAT evolution data were processed with TIGER least-squares models derived from the corresponding isotropic spectra as described in the Experimental Section. The TIGER technique is more fully described elsewhere.[5] Both PHORMAT and FIREMAT datasets for parthenolide utilized TPPM decoupling.[8]

Principal values for all 29 isotropically resolved carbons are included in Table 1. The reported data for the sp^3 carbons are obtained from the PHORMAT method, but despite the lengthy PHORMAT analysis, the S/N of the sp^2 carbons was insufficient for accurate analysis. Hence, the reported principal values for sp^2 carbons are taken solely from the FIREMAT analysis. While this shortcoming of PHORMAT limits the analysis of carbon peaks with broad powder patterns, unpublished work in our lab has established that near static patterns provide greater accuracy

(8) (a) Bennett, A. E.; Reinstra, C. M.; Auger, M.; Lakshmi, K. V.; Griffen, R. G. *J. Chem. Phys.* **1995**, *103*, 6951. (b) McGeorge, G.; Alderman, D. W.; Grant, D. M. *J. Magn. Reson.* In press.

(9) (a) Dunkel, R.; Mayne, C. L.; Curtis, J.; Pugmire, R. J.; Grant, D. M. *J. Magn. Reson.* **1990**, *90*, 290. (b) Dunkel, R.; Mayne, C. L.; Pugmire, R. J.; Grant, D. M. *Anal. Chem.* **1992**, *62*, 3133.

(10) Dixon, W. T. *J. Chem. Phys.* **1982**, *77*, 1800.

(11) Quick, A.; Rogers, D. *J. Chem. Soc., Perkin Trans. 2* **1976**, 465.

Table 1. Principal Values for Parthenolide and Corresponding Theoretical Values

C no.	chemical shift, experiment (theory)[a]				
	δ_{11}	δ_{22}	δ_{33}	δ_{iso}[b]	δ_{soln}[c]
	molecule 1				
1[d]	217.5 (222.9)	113.8 (117.0)	46.9 (50.1)	126.0 (130.0)	125.2
2	38.5 (42.5)	19.2 (21.3)	17.4 (16.1)	25.0 (26.6)	24.2
3	51.6 (55.9)	40.9 (44.6)	16.9 (19.7)	36.5 (40.1)	36.4
4	111.9 (108.4)	43.8 (42.8)	29.3 (26.3)	61.7 (59.2)	61.6
5	101.2 (102.1)	65.9 (65.5)	28.9 (23.7)	65.1 (63.8)	66.4
6	110.8 (111.0)	90.8 (87.0)	51.8 (46.1)	84.5 (81.4)	82.5
7	54.7 (55.6)	44.3 (46.9)	40.7 (44.0)	46.5 (48.8)	47.6
8	45.4 (50.3)	33.1 (32.8)	18.8 (17.2)	32.4 (33.4)	30.7
9	54.1 (53.6)	48.1 (51.0)	29.7 (30.7)	43.9 (45.1)	41.2
10[d]	241.3 (240.3)	140.4 (139.5)	31.7 (32.1)	137.7 (137.3)	134.7
11[d]	249.4 (254.3)	138.7 (136.5)	126.3 (126.7)	171.4 (172.5)	169.3
12[d]	235.6 (234.6)	128.3 (132.0)	57.3 (59.5)	140.4 (142.0)	139.3
13[d]	225.2 (226.2)	128.7 (126.7)	16.4 (15.2)	123.3 (122.7)	121.2
14	29.1 (27.8)	21.5 (21.1)	2.9 (−2.0)	17.8 (15.6)	17.3
15	31.6 (33.5)	16.3 (14.5)	5.1 (2.7)	17.6 (16.9)	17.0
	molecule 2				
1[d]	214.2 (218.6)	107.4 (113.6)	51.3 (50.7)	123.3 (127.6)	125.2
2	39.5 (43.5)	19.4 (19.5)	16.9 (16.3)	25.3 (26.4)	24.2
3	51.6 (49.5)	40.9 (41.7)	16.9 (17.6)	36.5 (36.3)	36.4
4	112.3 (114.8)	45.7 (42.7)	30.1 (31.8)	62.7 (63.1)	61.6
5	102.4 (101.8)	70.6 (66.3)	30.7 (35.2)	67.9 (67.8)	66.4
6	109.3 (107.7)	89.6 (85.8)	48.5 (46.2)	82.4 (79.9)	82.5
7	55.8 (57.7)	48.8 (49.3)	45.1 (45.6)	49.8 (50.9)	47.6
8	42.8 (47.8)	29.9 (32.5)	18.7 (16.2)	30.5 (32.2)	30.7
9	51.4 (55.0)	47.6 (50.5)	27.1 (28.7)	42.0 (44.7)	41.2
10[d]	238.1 (238.9)	135.6 (140.3)	30.5 (28.7)	134.7 (136.0)	134.7
11[d]	245.9 (246.6)	136.3 (136.4)	129.2 (122.2)	170.4 (168.4)	169.3
12[d]	235.9 (226.2)	126.1 (128.1)	58.6 (58.6)	140.1 (137.6)	139.3
13[d]	222.8 (215.2)	122.1 (118.6)	19.4 (14.6)	121.4 (116.1)	121.2
14	33.4 (30.0)	24.6 (23.6)	2.3 (−1.0)	20.0 (17.5)	17.3
15	32.4 (34.0)	16.3 (14.2)	5.5 (2.9)	18.1 (17.0)	17.0

[a] Theoretical tensor values, given in parentheses, calculated by using the B3PW91 method and 6-31+G (2d, p) basis. The structure used consisted of X-ray positions for heavy atoms and B3LYP/6-31G** refined hydrogen positions. [b] Isotropic experimental shifts obtained from a separate CP/MAS experiment. Theoretical isotropic values computed from the average of calculated principal values. [c] Solution values obtained from 2D INADEQUATE. [d] Principal values for these carbons were obtained from the FIREMAT analysis described. All other values are derived from PHORMAT data.

in all three principal values other factors being equal.[12] It is therefore desirable to use the high-quality PHORMAT principal values for aliphatic carbons when the inherently narrower powder patterns exhibit adequate S/N. While all reported aliphatic principal values are thus derived from PHORMAT data, the corresponding FIREMAT data differ by only ±0.95 ppm from the sp^3 values given in Table 1.

The better S/N in the FIREMAT experiment provided much more reliable principal values for sp^2 carbons. This experiment has two advantages over the corresponding PHORMAT data. First, PHORMAT requires that the magnetization be repeatedly restored to the *z*-axis during the pulse sequence by flip-back pulses.[3] These pulses significantly reduce the total magnetization remaining when the FID is acquired. By avoiding such pulses, the FIREMAT sequence retains more of the transverse magnetization. The second FIREMAT improvement results from acquiring the data with very few evolution increments (16 in the case of parthenolide). Portions of the acquisition data, corresponding to multiples of the period of the slow magic angle turning, are replicated and then rearranged to create a much larger data table for the evolution dimension with a concomitant improvement in the resolution in this dimension. The FIREMAT analysis provided data with S/N sufficient for accurate analysis of all sp^2 carbons in less than one-sixth of the time required for the PHORMAT analysis. The actual time saved is even greater, as the corresponding PHORMAT dataset had insufficient S/N for accurate analysis. Hence, the two datasets are not quite comparable. A comparison of PHORMAT and FIREMAT data for several representative olefinic carbons is presented in Figure 2 to illustrate the S/N differences typically found for sp^2 powder patterns which spread over a larger spectral range.

The acquisition of both PHORMAT and FIREMAT data for all carbons provides an opportunity to evaluate experimentally the similarities and differences of the two sets of principal shift values. Access to both measurements also resolves some of the controversy that has developed between those stressing the benefits and limitations of analysis using full powder bands versus spinning sidebands. Emsley has indicated that the greater S/N of axially symmetric tensors gives a better anisotropy and consequently the span ($\delta_{11}-\delta_{33}$) using sideband methods.[13] Emsley's analysis further concludes that the asymmetry parameter is optimally obtained from static patterns; this conclusion agrees with recent Monte Carlo analysis in our laboratory.[12] The Monte Carlo results demonstrate that for general tensor patterns (i.e., three different principal values) the near-static patterns of PHORMAT are more accurate providing sufficient S/N is available. As the δ_{11}, δ_{22}, and δ_{33} tensor components are unobtainable from the isotropic and anisotropy parameters alone (except for axially symmetric tensors), these results clarify that the distinct advantages claimed for sideband methods apply only to characterization of axially symmetric tensors and not necessarily all three tensor principal values.

The parthenolide principal shift data from the two independent experimental measurements were compared by determining the root-mean-square (rms) distance between corresponding principal values.[14] This distance between two tensors is defined as the integral of radial differences between the ellipsoidal surfaces representing the shift tensors. A comparable rms deviation computed solely from differences in the three principal values depends only on the three points in the Cartesian representation where the principal axes intersect the ellipsoidal surface. It is claimed that the surface integral approach compares principal values in a more reliable manner.[14] For the carbons in parthenolide, a rms distance of ±0.95 ppm was found between PHORMAT and FIREMAT data. This value is comparable to the intrinsic experimental measurement errors of both approaches. Hence, the principal values determined from either method appear to be reliable.

^{13}C Chemical Shift Assignments. Although chemical shift principal values have been demonstrated to be extremely sensitive to molecular geometry, before structural relationships can be identified, it is critical that the tensor bands for the various isotropic shifts first be correctly assigned to their respective carbons. Recently, an approach was outlined in which high-quality ab initio calculated principal values were used to assign all solid-state shifts in caryophyllene oxide, a 15 carbon terpene.[6] This approach includes a statistical confidence level to assess the reliability of each shift assignment.

The doubling of all but one degenerate pair of lines in parthenolide arises from the presence of two conformationally similar molecules per asymmetric unit. To assign shifts, pairs of lines arising from the same carbon in the two slightly different crystal environments must first be identified. Correct pairing usually is easily recognized by inspection of a contour plot of the PHORMAT spectrum. Since the two lines in a pair represent

(12) Alderman, D. W.; Grant, D. M. 39th Experimental NMR Conference, 1998; poster 13, session 2.
(13) Hodgkins, P.; Emsley, L. *J. Chem. Phys.* **1997**, *107*, 4808.
(14) Alderman, D. W.; Sherwood, M.; Grant, D. M. *J. Magn. Reson., Ser. A* **1993**, *101*, 188.

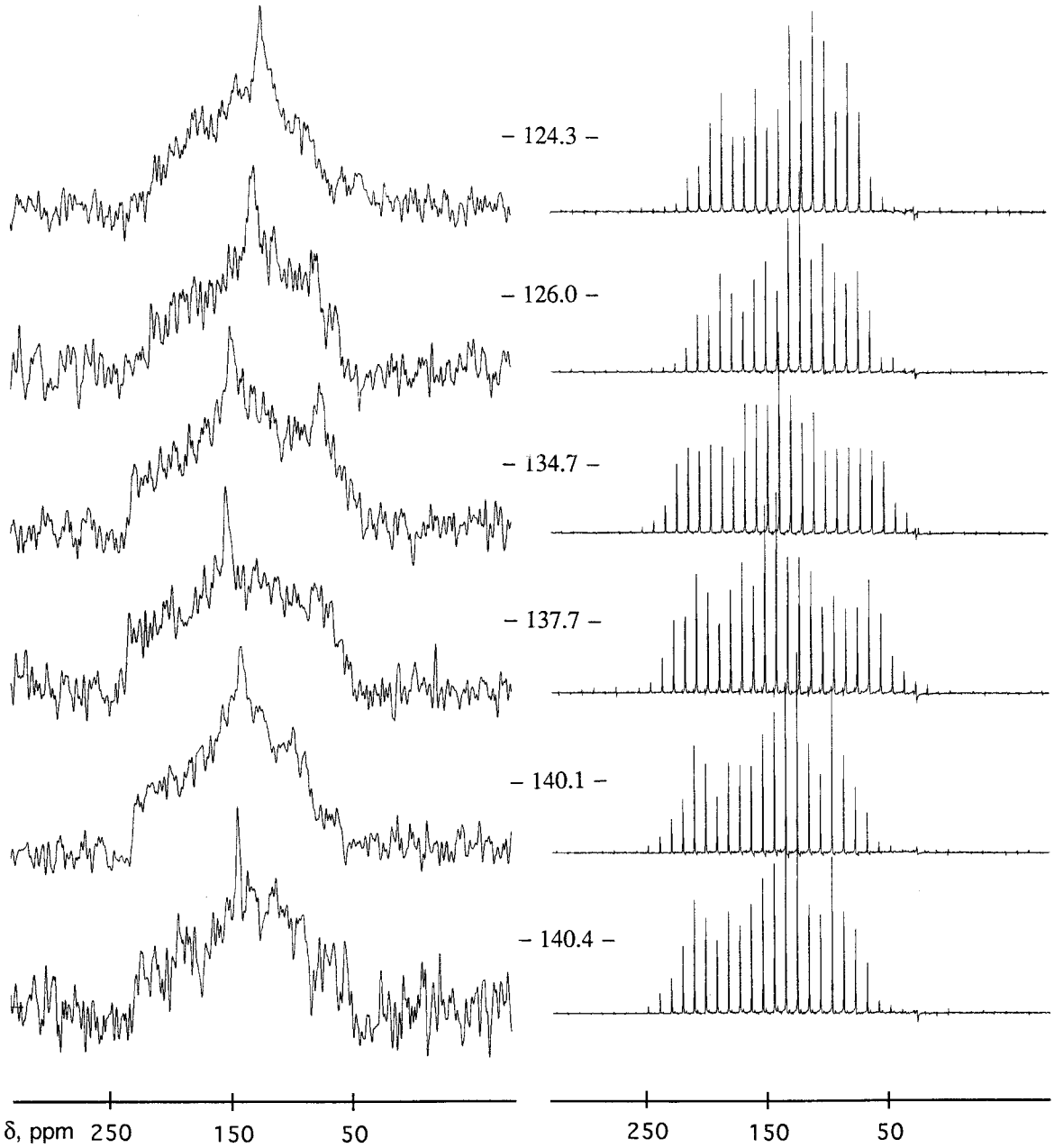

Figure 2. A comparison of the S/N for sp^2 carbons obtained from PHORMAT (left) and FIREMAT (right) analyses. The superior S/N of the FIREMAT data was achieved in an experiment requiring only 15% of the PHORMAT analysis time as a result of the unique data rearrangement and processing methods described.

the same molecular position in slightly different conformational or crystallographic environments, the two isotropic shifts tend to be very similar. The corresponding powder patterns also exhibit comparable spans and skews. In Figure 3 a representative contour plot illustrates the obvious similarities of five pairs of tensor bands. For most of parthenolide's carbon resonances, the isotropic lines provide equally distinct pairing information. However, for the overlapping methyl lines at 17.6−20.0 ppm it is unclear what the pairing should be. The TIGER derived powder patterns for this region (shown in Figure 4) use information from a separate high-resolution guide spectrum to clearly identify the lines at 17.8 and 20.0 ppm as arising from the same molecular position, while those at 17.6 and 18.1 ppm are similarly associated. This pairing illustrates the additional benefits of tensor shifts over isotropic shifts for this initial step in shift assignment and demonstrates the unique abilities of TIGER processing.

While this line pairing identifies the two isotropic shifts arising from the same type of carbon (i.e., carbons with the same numbering as shown in Figure 1), it fails to identify the specific molecular position associated with a given pair of similar bands. Furthermore, such pairing lacks direct information regarding the specific molecule in the asymmetric unit to which a given line should be assigned.

A complete shift assignment requires the following two steps. First, each *pair* of lines in the asymmetric unit must be assigned to a specific molecular position. Second, each *individual* line in a given pair must then be associated with one of the two unique molecules in the lattice. The initial process involves computing ab initio tensors for a diffraction structure with use of established methods. From the correlation of experimental principal shifts versus calculated shieldings the best assignment is made on the basis of the correlation coefficient (with no attempt to differentiate between the two carbons of the same

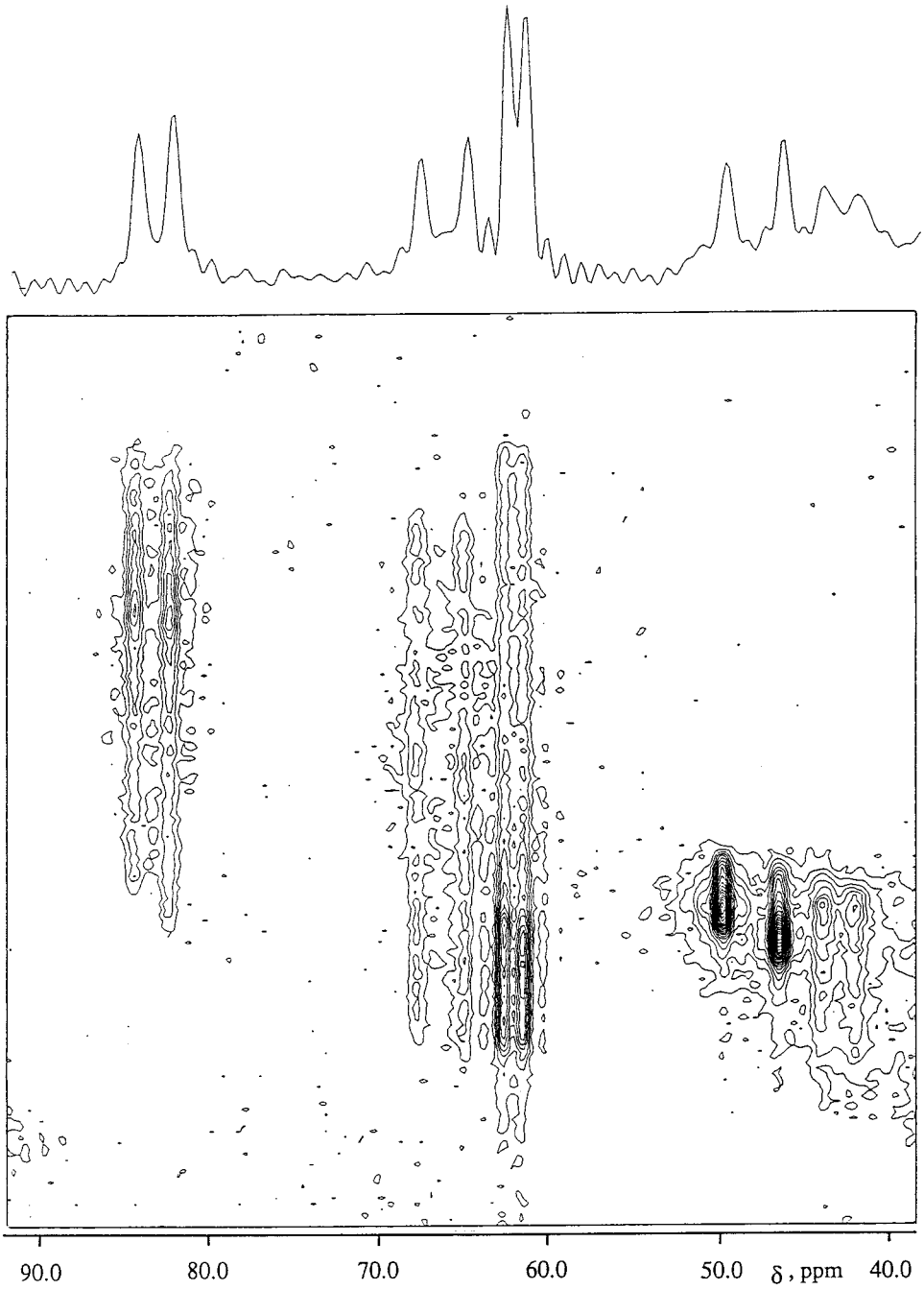

Figure 3. PHORMAT contour map exhibiting obvious pairing of carbon lines arising from the same molecular position in the two unique molecules of the asymmetric unit.

type). On the basis of a statistical assessment of the errors, Gaussian confidence intervals are established as the criteria for distinguishing between alternative assignments.[6] These tensor computational methods, outlined below, provided reliable assignments of all pairs of parthenolide lines to specific molecular positions. However, the assignment of a given carbon line to one of the distinct molecules in the crystallographic asymmetric unit is more challenging.

Associating an individual carbon with a distinct molecule in the asymmetric unit usually is impossible with conventional isotropic NMR techniques. Paired carbons normally have not only very close isotropic shifts but also similar relaxation properties as they represent the same carbon type in slightly different environments. However, these carbon pairs often differ in the relative orientations of the shift tensor to the local crystallographic environment of the asymmetric unit. Hence, single-crystal data normally reveal these directional differences. In some powders, the differences in conformational and electronic environments of different molecules in an asymmetric unit, while small, are sufficiently unique that comparisons with computed shift tensor values allow these subtle distinctions between carbon pairs to be made despite the absence of directional information. By considering alternative pairings of the experimental values for a specific pair of carbons with computed carbon tensors, a correlation coefficient is computed for each assignment permutation. The arrangement with the highest correlation coefficient is then selected as the most likely individual pairing, even though several pairings do not provide statistically significant differences. The overall best assignment for the entire molecule is the combination of the set of best individual pairings. A statistical confidence level is then derived from the agreement between the theoretical and experimental

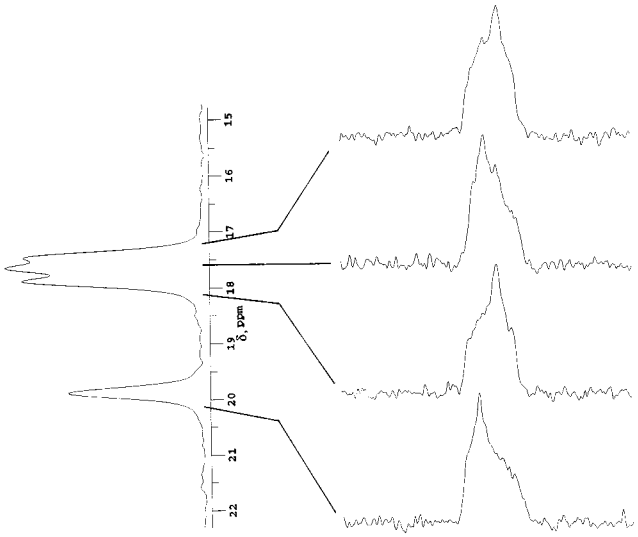

Figure 4. TIGER-derived powder patterns for the methyl carbons 14 and 15. Correctly identifying pairs of lines arising from the same carbon in the two molecules in the crystallographic asymmetric unit is impossible with use of only isotropic shift as shown in the spectrum on the left side of the figure. In contrast, the powder patterns clearly identify the peaks at 17.6 and 18.1 ppm as arising from the same molecular position. The lines at 17.8 and 20.0 ppm are also obviously paired.

values for the entire molecule and this value provides a figure of merit for estimating the most favored assignment.

Such comparisons for parthenolide yielded assignments with reasonably high statistical confidence (i.e., the >90% confidence level corresponding to ±3.75 ppm for aliphatic carbons and ±5.23 ppm for olefinic carbons). Of the 15 total carbon pairs, seven fell above this confidence level (carbons 1, 7, 8, 9, 11, 13, and 14). Two additional carbons (5 and 10) were assignable at roughly the 70% confidence level. Unfortunately, carbons 2, 4, 6, 12, and 15 failed to exhibit a significant statistical preference for one pairing over the alternate permutation. In the case of carbon 3 the two lines are isotropically degenerate, and thus such an association is actually irrelevant. In those cases where there was no clear best assignment, the tentative designations shown in Table 1 are those with the highest correlation coefficient. This work on parthenolide represents the first assignment of NMR shifts to distinct molecules in the crystallographic asymmetric unit and demonstrates pointedly the value of tensor principal values in some ^{13}C chemical shift studies.

Comparison of Quantum Mechanical Methods. Before a comparison of theoretical methods can be discussed, a brief description of the methods and abbreviations is given. The BLYP and BPW91 methods are both density functional methods. Both use Becke's 1988 exchange functional[15] together with the correlation functional of either Lee et al.[16] in the case of BLYP or Perdew and Wang[17] in the case of BPW91. The B3LYP and B3PW91 methods are hybrid methods including contributions from both Hartree−Fock and density functional theory and use the respective correlation functionals, described above, together with Becke's three-parameter exchange functional.[18] All shielding tensors were computed with Gaussian 94[19] run on IBM SP computers with parallel processing techniques. Tensor computations used the gauge-including atomic orbital (GIAO) method.[20]

(15) Becke, A. D. *Phys. Rev. A* **1988**, *38*, 3098.
(16) Lee, C.; Yang, W.; Parr, R. G. *Phys. Rev. B* **1988**, *37*, 785.
(17) Perdew, J. P.; Wang, Y. *Phys. Rev. B* **1992**, *45*, 13244.
(18) Becke, A. D. *J. Chem. Phys.* **1993**, *98*, 5648.

Table 2. Comparison of Tensor Computation Methods for Parthenolide

	HF	BLYP	BPW91	B3LYP	B3PW91	B3PW91[a,b]
			aliphatic			
error (rms dist.)	2.5	2.4	2.2	2.2	2.0	2.3
slope	−0.94	−1.04	−1.05	−1.03	−1.03	−0.98
intercept	199.61	186.96	183.4	187.5	190.4	192.4
			sp^2 carbons			
error (rms dist.)	4.9	4.7	4.4	3.7	3.5	3.2
slope	−1.15	−0.96	−0.95	−1.00	−1.01	−0.98
intercept	219.55	187.80	184.71	192.5	194.9	197.4

[a] Tensor values computed with the 6-31+G (2d, p) basis set. All other reported values were computed with the D95** basis. [b] The increase in sp^3 error with a larger basis is assumed to be due to the large number (i.e.,50%) of sp^3 carbons unassignable in the asymmetric unit and is considered a more accurate reflection of the true error.

Previous evaluations of shift computation methods have usually focused on comparisons of only isotropic components.[21] However, principal values offer a more accurate comparison as individual values are associated with specific electronic and structural features. Hence, failures in computational models are more readily recognized from principal values.

In our previous analysis the two sp^2 hybridized carbons in caryophyllene oxide were insufficient in number to establish generalizations characterizing tensors for such carbons.[6] The presence of 10 sp^2 carbons (i.e., five pairs) from parthenolide now provides a sufficiently large data set for a more systematic assessment of sp^2 carbon shifts. Five tensor computational methods were examined by using the X-ray determined heavy atom positions along with a B3LYP/6-31G* refinement of the proton positions. Such optimization of proton positions yields C−H bond lengths more consistent with neutron diffraction analyses[22] and 2-fold improvements in the tensor fits.[6,22] Parthenolide's computed shieldings were correlated with experimental shifts by using slope and intercept values obtained with standard least-squares methods. Separate slope and intercept parameters were used for sp^2 and sp^3 carbons as the computed sp^2 values are known to suffer differentially from inaccuracies due to electron correlation not found in sp^3 carbons. Results of this comparison are exhibited in Table 2 and demonstrate that the B3PW91 method yields tensors which best match the parthenolide data. Analysis with the larger 6-31+G (2d, p) basis provides further improvement in computed sp^2 tensor values and hence B3PW91/6-31+G (2d, p) tensors were used in making the final shift assignments in this work.

For computed aliphatic shifts, the B3PW91 method also provided the best fit consistent with our previous statistical evaluation. However, saturated carbons are less sensitive to the specific theoretical method used and all of the computations yield statistically comparable sp^3 tensors.

(19) *Gaussian 94* (Revision A.1), Frisch, M. J.; Trucks, G. W.; Schlegel, H. B.; Gill, P. M. W.; Johnson, B. G.; Robb, M. A.; Cheeseman, J. R.; Keith, T. A.; Petersson, G. A.; Montgomery, J. A.; Raghavachari, K.; Al-Laham, M. L.; Zakrzewski, V. G.; Ortiz, J. V.; Foresman, J. B.; Cioslowski, J.; Stefanov, B. B.; Nanayakkara, A.; Challacombe, M.; Peng, C. L.; Ayala, P. Y.; Chen, W.; Wong, M. W.; Andres, J. L.; Replogle, E. S.; Gomperts, R.; Martin, R. L.; Fox, D. J.; Brinkley, J. S.; Defrees, D. J.; Baker, J.; Stewart, J. P.; Head-Gordon, M.; Gonzalez, C.; Pople, J. A. Gaussian, Inc.: Pittsburgh, PA, 1995.
(20) Ditchfield, R. *Mol. Phys.* **1974**, *27*, 789.
(21) (a) Cheeseman, J. R.; Trucks, G. W.; Keith, T. A.; Frisch, M. J. *J. Chem. Phys.* **1996**, *104*, 5497. (b) Gauss, J. *J. Chem. Phys.* **1993**, *99*, 3629.
(22) (a) Liu, F.; Orendt, A. M.; Alderman, D. W.; Grant, D. M. *J. Am. Chem. Soc.* **1997**, *119*, 898. (b) Liu, F.; Phung, C. G.; Alderman, D. W.; Grant, D. M. *J. Am. Chem. Soc.* **1996**, *118*, 10629.

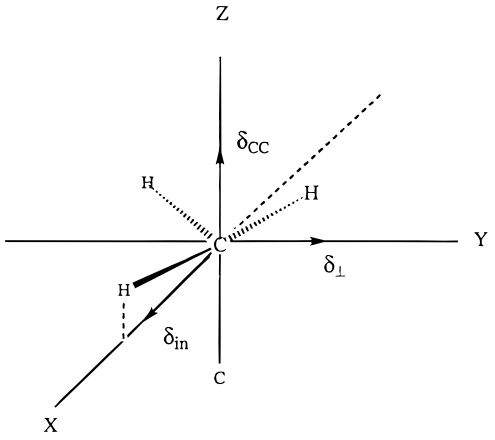

Figure 5. Characteristic orientations of chemical shift tensor principal axes in methyl groups. Minor variations in orientations of these axes occur as local symmetry varies.

The quality fit of computed tensors to experimental values has an interesting implication. Previous studies of polymorphism have usually suggested that NMR solid-state shift differences between polymorphs result from differences in the surrounding lattice structure.[23] As parthenolide's calculated tensors accurately reflect the experimental values for two conformationally different molecules with no consideration of the intermolecular lattice features, it would appear that even minor conformational differences become dominant factors influencing nuclear shielding. Apparently, in parthenolide, intermolecular lattice interactions become important only to the extent that they alter the molecular conformation. The dominance of conformation effects appears to be quite general as previous theoretical assessments of carbohydrates,[22,24] terpenes,[6] and aromatics[25] also provided accurate tensor values while ignoring lattice effects. Undoubtedly as theoretical methods improve, the inclusion of direct lattice shielding effects may yet improve these calculations, but intermolecular effects tend to be small, except when strong intermolecular associations such as hydrogen bonds are present.[26]

Methyl Shift Tensors. The ability to assign isotropic shifts accurately expands the opportunity to study the effects of various subtle structural factors on principal shift values. Previously we have shown that methyl principal values reflect steric interactions with proximate molecular moieties.[6] A single shift component, $\delta_\perp$, (orientational designations of shift components in the CH_3 molecular frame are shown in Figure 5), was observed to move to lower frequencies or higher fields when one of the methyl hydrogens is less than the van der Waal distance from a perturbing proton. The origin of these variations in principal values and the specifics regarding their orientations must rely on computed shift tensors as experimental principal values obtained from powders lack directional information.

Relative to a sterically unperturbed methyl, two of parthenolide's methyl principal values, $\delta_\perp$ and δ_{in}, were found to move to lower frequencies or higher fields with steric interactions present. These two components are both oriented perpendicular to the triad methyl axis. This shift to higher fields occurs in both methyls in each of the two molecules found in the asymmetric unit. These shifts to higher fields are graphically portrayed in Figure 6 along with principal values from caryophyllene oxide (structure shown in Figure 7) and 1,1-dimethyl cyclohexane, included for comparison. In all cases, the δ_{CC} component tends to remain least affected by steric perturbations. These significant changes in the $\delta_\perp$ and δ_{in} shift components have been previously observed[6,29] and an explanation is provided by well-established principals governing chemical shifts.

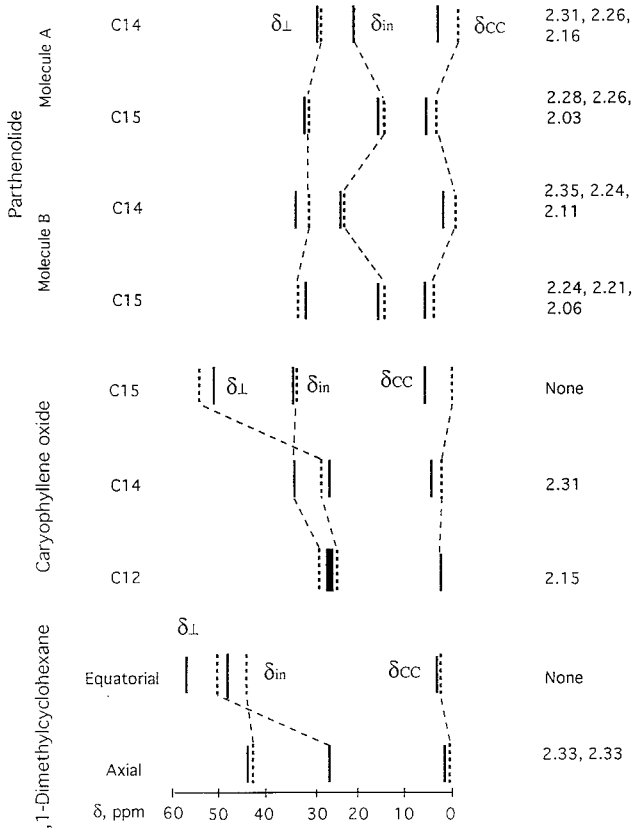

Figure 6. Theoretical (···) and experimental (—) methyl principal values for parthenolide. Values for caryophyllene oxide and 1,1-dimethylcyclohexane are included for comparison. Distances from methyl protons to perturbing protons (i.e., those within 2.35 Å) are given in Å on the right side of the figure. All orientational designations are derived from theoretical tensors as such data are unavailable from principal values of powders. The tensors for both parthenolide and caryophyllene oxide were computed by using the B3PW91 method with the 6-31+G (2d, p) basis. Theoretical tensors for 1,1-dimethylcyclohexane were computed as described in ref 29.

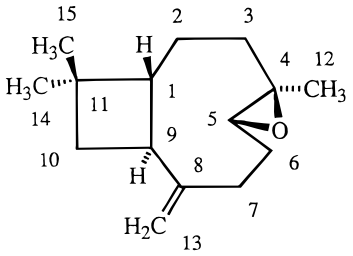

Figure 7. Structure of caryophyllene oxide.

(23) (a) Fletton, R. A.; Lancaster, R. W.; Harris, R. K.; Kenwright, A. M.; Packer, K. J.; Waters, D. N.; Yeadon, A. *J. Chem. Soc., Perkin Trans. 2* **1986**, 1705. (b) Byrn, S. R.; Pfeiffer, R. R.; Stephenson, G.; Grant, D. J. W.; Gleason, W. B. *Chem. Mater.* **1994**, *6*, 1148.

(24) Liu, F.; Phung, C. G.; Alderman, D. W.; Grant, D. M. *J. Magn. Reson., Ser. A* **1996**, *120*, 242.

(25) (a) Orendt, A. M.; Hu, J. Z.; Jiang, Y. J.; Faccelli, J. C.; Wang, W.; Pugmire, R. J.; Ye, C.; Grant, D. M. *J. Phys. Chem., A* **1997**, *101*, 9169. (b) Facelli, J. C.; Orendt, A. M.; Jiang, Y. J.; Pugmire, R. J.; Grant, D. M. *J. Phys. Chem.* **1996**, *100*, 8268.

(26) (a) Zheng, G.; Wang, L.; Hu, J.; Zhang, X.; Shen, L.; Ye, C.; Webb, G. A. *Magn. Reson. Chem.* **1997**, *35*, 606. (b) Facelli, J. C.; Pugmire, R. J.; Grant, D. M. *J. Am. Chem. Soc.* **1996**, *118*, 5488.

(27) Facelli, J. C. In *Encyclopedia of NMR*; Grant, D. M., Harris, R. K., Eds.; Wiley: Chichester, 1996; Vol. 7, pp 4299−4306.

(28) Duncan, T. M. In *A Compilation of Chemical Shift Anisotropies*; Farragut: Chicago, 1990; pp C5−C9. (b) Veeman, W. S. *Prog. Nucl. Magn. Reson. Spectrosc.* **1984**, *16*, 193.

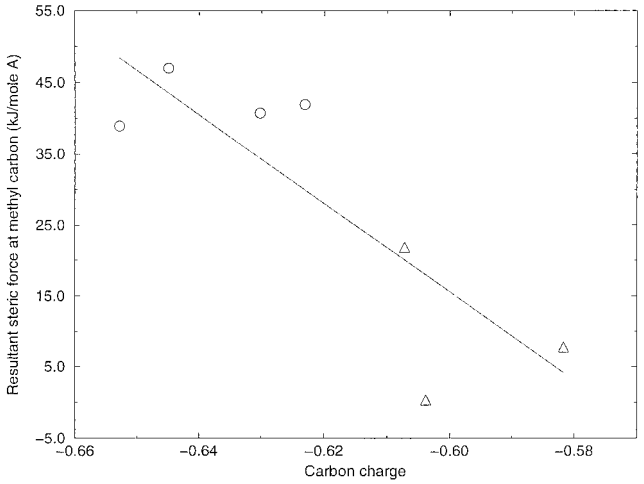

Figure 8. Electronic charges on methyl carbons versus resultant hydrogen steric forces affecting the perturbed carbon through methyl C−H bonds. Methyls from parthenolide (○) and caryophyllene oxide (△) are both included for a more statistically significant comparison. The correlation coefficient is −0.84 for these data. All charges were computed by using the B3LYP method with the 6-31G* basis.

Previous perturbation treatment of the chemical shift[27] has established that principal shift components change as a result of variations in several molecular properties. For a given atom, shielding arises from the circulation of electrons in planes perpendicular to the designated principal axes. This electronic circulation is inversely related to the difference in the energy, $1/\Delta E$, between the bonding, σ, and antibonding, σ^*, molecular orbitals which are mixed by a magnetic field.[1] The shift also depends on the average inverse cubic distance, $\langle 1/r^3 \rangle$, of the screening electrons from the nucleus. For methyl groups, the ΔE between σ and σ^* for a C−CH_3 bond is less than that of a C−H bond consistent with the less energetic C−C bond. Hence, the more significant field induced electron circulation currents involve C−CH_3 σ bonds. As $\delta_\perp$ and δ_{in} are directed perpendicular to this bond, these components exhibit the greatest sensitive to variations in C−CH_3 bond electron densities and their energetics. This conclusion is further supported by the near invariance of the δ_{CC} (invariably the δ_{33} shift component) found in numerous analyses of methyl principal values.[28] This tensor component strongly reflects electronic variation in the C−H bonds, as it primarily lies parallel to the methyl C−C bond. Hence, the minimal δ_{CC} variation is evidence that electronic currents involving the C−CH_3 bond dominate changes in methyl shielding tensors.

The relationship between steric forces on the methyl hydrogens and direction of movement in the δ_{in} and $\delta_\perp$ components to lower frequencies or higher fields is partially explained by the $\langle 1/r^3 \rangle$ term. As steric forces at the methyl carbon increase, the computed negative charge increases on the carbon of interest as shown in Figure 8. This electronic charge buildup causes the effective distance r to increase due to electronic repulsion consistent with Slater screening rules for electrons on the same atom. The Slater screening rules may be used to calculate the effective nuclear charge and, therefore, to estimate the changes in the inverse cubic distance. As the shift depends directly on $\langle 1/r^3 \rangle$, a larger r results in a smaller paramagnetic term and an upfield shift of the δ_{in} and $\delta_\perp$ components.

While steric forces can potentially shift both perpendicular components, previous studies have determined that the change in the $\delta_\perp$ component is usually the largest (see Figure 6)[6,29] when only one hydrogen of a CH_3 is sterically impacted. A single unique hydrogen thus also defines the direction of the δ_{in} axis. As the perturbed C−H bond and adjacent C−C bond define a plane perpendicular to the $\delta_\perp$ direction, it is the $\delta_\perp$ component that is altered more than δ_{in}. Conversely, the perturbed C−H bond experiences very little of the steric force in a direction perpendicular to the H−C−C plane. Hence, such symmetry constraints result in smaller variation of this δ_{in} component relative to the $\delta_\perp$. Thus, when only one hydrogen of a CH_3 is perturbed, the $\delta_\perp$ component dominates the shift variation. When two or more of the methyl hydrogens are sterically perturbed, the δ_{in} and $\delta_\perp$ designations become somewhat ambiguous and both components contribute significantly to variations in the chemical shielding. Hence, the magnitude of variation in the two perpendicular modes depends on the relative extent that two or more of the methyl protons are perturbed. In parthenolide both δ_{in} and $\delta_\perp$ are shifted upfield, indicating that more than one methyl hydrogen is significantly sterically perturbed. Similar steric features obtain for other carbon types but are not treated here as they are less easily visualized than methyl shifts. As the theoretical results mirror the experimental trends in shift tensors, the experimental shift data validate the accuracy of the molecular wave functions.

Conclusions

Previously, the characterization of natural abundance ^{13}C principal shift values for all carbons in moderately large molecules was difficult or impossible. Here, the PHORMAT and FIREMAT analyses combine to provide an excellent set of principal shifts for all of the 29 isotropic lines in the parthenolide ^{13}C spectrum. FIREMAT has been shown to agree with high-quality PHORMAT data and constitutes an especially valuable way to acquire accurate sp^2 principal values that are difficult to obtain in powder samples. Comparable sp^2 values from PHORMAT require spectral intensities obtainable only with prohibitively long data acquisitions. In this study we pursued a two-experiment approach in which sp^3 principal values were obtained from both PHORMAT and FIREMAT to assess the relative accuracy of the two methods. Fortunately, the close match of the PHORMAT and FIREMAT sp^3 values suggests that the time savings and increased sensitivity of FIREMAT make it the preferable method for moderately large molecules and validates the sole use of FIREMAT data for sp^2 shifts.

Analysis of parthenolide provided principal values for 10 sp^2 carbons. This expanded set of tensor data allows a more detailed evaluation of computational methods in sp^2 carbons than possible from our previous study of caryophyllene oxide.[6] As in the former study the B3PW91 tensor computation provides the best match to computed tensors with standard deviations of ±2.3 ppm for aliphatic carbons and ±3.2 ppm for olefinic carbons.

The ability to assign carbon shifts to separate molecules in the asymmetric unit, as demonstrated here, indicates that modern tensor computational methods are now of sufficient quality to monitor relatively minor conformational changes in structure. This sensitivity of ^{13}C shift tensors is, perhaps, best reflected by our ability to assign 9 of parthenolide's congruent pairs arising from the 15 total shift pairs in the asymmetric unit of the finely divided powder. This differentiation is achieved despite the fact that the surrounding bond lengths and angles for corresponding carbon atoms typically differed by only a few hundredths of an angstrom or a few degrees, respectively.

(29) Soderquist, A.; Facelli, J. C.; Horton, W. H.; Grant, D. M. *J. Am. Chem. Soc.* **1995**, *117*, 8441.

Chemical shift tensors have been known for some time to be extremely sensitive to molecular structure.[30] Hence, these shift variations in methyl tensors have implications for conformational studies in noncrystalline solids. Here it is demonstrated that methyl tensor shifts strongly reflect steric perturbations. Further, the upfield movement of either one or two of the perpendicular components specifies whether one or more hydrogens are influenced sterically. Such data provide crucial information in choosing between alternative computer-generated model structures. Shift tensors of carbon types other than methyls are equally promising and future analyses should eventually provide a larger foundation for more detailed and accurate solid-state structure characterization from powder data.

Acknowledgment. Computer resources for tensor computations were provided by the Center for High Performance Computing at the University of Utah. We thank Dr. D. W. Alderman for assistance in fitting the PHORMAT and FIREMAT data and TIGER processing both datasets. Funding for this research was provided by NIH grant GM 08521-37.

JA990251B

(30) Facelli, J. C.; Grant, D. M. *Top. Stereochem.* **1989**, *19*, 1.